

# Lawrence Berkeley National Laboratory

## Recent Work

### Title

NORMAL PHOTOELECTRON DIFFRACTION OF  $c(2 \times 2)0(1s)$ -Ni(001) AND  $c(2 \times 2)S(2p)$ -Ni(001),  
WITH FOURIER TRANSFORM ANALYSIS

### Permalink

<https://escholarship.org/uc/item/02c3g4r6>

### Author

Rosenblatt, D.H.

### Publication Date

1980-09-01



# Lawrence Berkeley Laboratory

UNIVERSITY OF CALIFORNIA

## Materials & Molecular Research Division

RECEIVED  
LAWRENCE  
BERKELEY LABORATORY

NOV 20 1980

Submitted to Physical Review B

LIBRARY AND  
DOCUMENTS SECTION

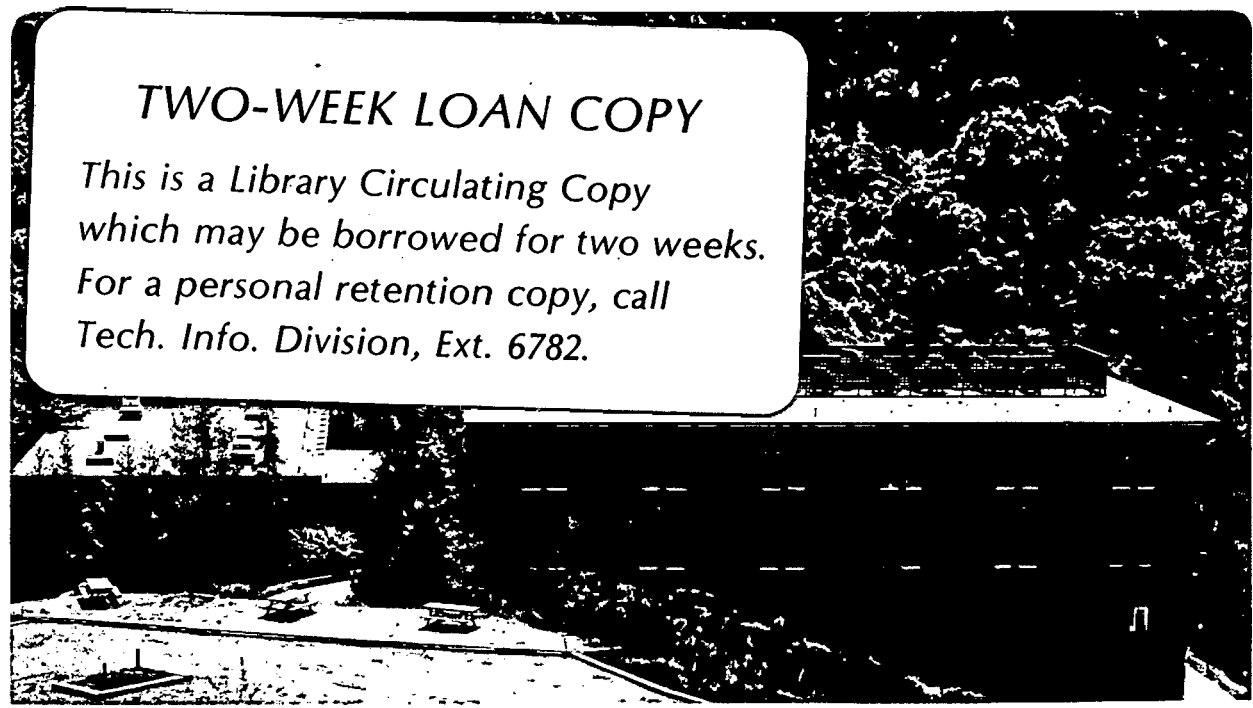
NORMAL PHOTOELECTRON DIFFRACTION OF  $c(2 \times 2)0(1s)$ -Ni(001) AND  
 $c(2 \times 2)S(2p)$ -Ni(001), WITH FOURIER TRANSFORM ANALYSIS

D.H. Rosenblatt, J.G. Tobin, M.G. Mason, R.F. Davis,  
S.D. Kevan, D.A. Shirley, C.H. Li and S.Y. Tong

September 1980

### TWO-WEEK LOAN COPY

*This is a Library Circulating Copy  
which may be borrowed for two weeks.  
For a personal retention copy, call  
Tech. Info. Division, Ext. 6782.*



LBL-11447 c. 2

## **DISCLAIMER**

This document was prepared as an account of work sponsored by the United States Government. While this document is believed to contain correct information, neither the United States Government nor any agency thereof, nor the Regents of the University of California, nor any of their employees, makes any warranty, express or implied, or assumes any legal responsibility for the accuracy, completeness, or usefulness of any information, apparatus, product, or process disclosed, or represents that its use would not infringe privately owned rights. Reference herein to any specific commercial product, process, or service by its trade name, trademark, manufacturer, or otherwise, does not necessarily constitute or imply its endorsement, recommendation, or favoring by the United States Government or any agency thereof, or the Regents of the University of California. The views and opinions of authors expressed herein do not necessarily state or reflect those of the United States Government or any agency thereof or the Regents of the University of California.

NORMAL PHOTOELECTRON DIFFRACTION OF  $c(2 \times 2)0(1s)$ -Ni(001) AND  
 $c(2 \times 2)S(2p)$ -Ni(001), WITH FOURIER TRANSFORM ANALYSIS

D. H. Rosenblatt, J. G. Tobin, M. G. Mason,\* R. F. Davis,  
S. D. Kevan,\*\* D. A. Shirley

Materials and Molecular Research Division  
Lawrence Berkeley Laboratory

and

Department of Chemistry  
University of California  
Berkeley, California 94720

C. H. Li\*\*\* and S. Y. Tong

Department of Physics and Surface Studies Laboratory  
University of Wisconsin-Milwaukee  
Milwaukee, Wisconsin 53201

September 1980

---

\*Permanent address: Research Laboratory, Eastman Kodak, Rochester,  
NY 14650.

\*\*Permanent address: Bell Laboratories, Murray Hill, NJ 07974.

\*\*\*Permanent address: Department of Physics, National Tsing Hua  
University, Hsinchu, Taiwan, Republic of China.

## ABSTRACT

Normal photoelectron diffraction was used to study the structure of the  $c(2 \times 2)O$  and  $c(2 \times 2)S$  overlayers on Ni(001). The oxygen and sulfur atoms were found to lie above the fourfold hollow sites in the Ni(001) surface with  $d_{\perp}$  spacings of  $0.90 \pm 0.04 \text{ \AA}$  and  $1.30 \pm 0.04 \text{ \AA}$  respectively, where  $d_{\perp}$  is the perpendicular interplanar spacing between the adsorbate and surface layers. A Fourier transform analysis was carried out on the experimental data. In both cases, the modulus of the Fourier transforms gave two large peaks in the real-space/distribution function. The maxima of these peaks closely corresponded to  $d_{\perp} + b$  and  $d_{\perp} + 2b$ , where  $b$  is the interlayer spacing in Ni(001). The range of experimental data in  $k$ -space was not large enough to yield the value of  $d_{\perp}$  directly.

## I. INTRODUCTION

Normal photoelectron diffraction (NPD) shows promise as a method for accurate structure determinations of ordered overlayers of atoms<sup>1,2</sup> and molecules,<sup>3</sup> as well as of disordered atomic overlayers,<sup>2</sup> on metal surfaces. In an NPD experiment the photoemission intensity of an adsorbate core level is measured normal to the surface as a function of photon, and consequently photoelectron energy. The intensity-kinetic energy curve thus generated is compared to theoretical calculations to make the structure determination. Both experiment and theory bear resemblance to dynamical low energy electron diffraction (LEED), and for all systems in which both methods have been tried to date, the same structure has been obtained. However, existing NPD theories,<sup>4</sup> based on earlier LEED formalisms, require extensive calculations which thereby limit the method.

Recently, it has been suggested that NPD can be compared with extended x-ray absorption fine structure (EXAFS).<sup>4,5</sup> The important structural parameter in NPD, an angle-resolved experiment in which intensity data are taken normal to the crystal face, is  $d_{\perp}$ , the perpendicular spacing between the adsorbate layer and the surface layer, whereas EXAFS, an angle-integrated technique, yields the nearest neighbor distance  $R_{nn}$ . An inspection of the NPD curves calculated for a series of  $d_{\perp}$  distances shows that the peaks move to lower energies as  $d_{\perp}$  is increased, resulting in an increased frequency of the NPD oscillations.<sup>6</sup> The same effect is observed in EXAFS as a function of nearest neighbor distance, since the oscillations go as

$\sin(2kR_{nn})$ . This effect was also observed experimentally for the system  $p(2 \times 2)\text{Se-Ni}(001)$ , where a low temperature form (probably  $\text{H}_2\text{Se}$ ) causes a systematic shift in the NPD peaks.<sup>5</sup>

In this paper, we present NPD structure determinations of two additional atomic adsorbate systems, the  $c(2 \times 2)$  oxygen and sulfur overlayers on  $\text{Ni}(001)$ . Again we obtain the same results as the LEED intensity analyses. We also present additional experimental evidence that NPD is similar to EXAFS: We show that experimental NPD data can be Fourier transformed to directly yield interlayer distances along the surface normal.

Section II contains the experimental information. Section III presents NPD data and a discussion of the surface structures which are derived. In Section IV, the first application of the Fourier transform to experimental NPD data is reported. Section V gives some conclusions about this work.

## II. EXPERIMENTAL

All data reported here were obtained with an angle resolved photoemission (ARP) spectrometer, described elsewhere.<sup>7</sup> The spectrometer has low energy electron diffraction (LEED) and Auger electron spectroscopy (AES) capabilities, as well as an adsorbate introduction system which allows for both ambient dosing and effusive beam dosing. The nickel crystal was oriented to within  $1/2^\circ$  of the (001) face. It was cleaned by hot (1025 K) and room temperature cycles of argon ion sputtering followed by annealing to 875 K, resulting in a surface essentially clean of impurities with a sharp (1x1) LEED pattern. To obtain the c(2x2) oxygen overlayer, the crystal was exposed to an ambient pressure of  $2 \times 10^{-8}$  torr  $O_2$ . The LEED pattern was continuously monitored to ensure that a coverage of approximately 0.5 monolayer was obtained. Exposure was stopped at  $\sim 20$  Langmuirs, when the last evidence of p(2x2) spots disappeared and the c(2x2) pattern became sharp. This ensured a submonolayer coverage of c(2x2) oxygen. The c(2x2) sulfur overlayer was prepared by directing an effusive beam of  $H_2S$  at the nickel surface. Effusive beam dosing was used to maintain vacuum integrity. An exposure of 20-30 Langmuirs produced a sharp c(2x2) LEED pattern. All exposures of  $O_2$  and  $H_2S$  were made with the sample at 300 K. The base pressure of the chamber was  $2 \times 10^{-10}$  torr.

The experiments were performed on Beam Line I-1 at the Stanford Synchrotron Radiation Laboratory (SSRL). The oxygen experiment was done during a dedicated SSRL run, with a stored ring current of



45–90 mA. The high photon flux available with dedicated running was necessary because of the low photoemission cross section of the O(1s) level. Experiments in the region above the oxygen K-edge (binding energy 537 eV with respect to the vacuum level) are hampered by the high percentage of scattered light, the loss of intensity to absorption by carbon contamination on the optical elements, and the poor resolution of the grasshopper monochromator. The theoretical resolution of the monochromator with a 1200 line/mm grating installed is  $\Delta E = 8 \times 10^{-6} E^2$  (eV), or 3.1 eV at a photon energy of 620 eV. The O(1s) natural linewidth for this system at  $h\nu = 1487$  is known to be less than 1.5 eV.<sup>8</sup> The resolution of our electron analyzer is less than 0.5 eV at 80 eV pass energy. Assuming a 1.5 eV natural linewidth, a combination of these three factors should give an O(1s) peak width of about 3.5 eV. However, the observed FWHM for O(1s) in this experiment at 620 eV is 7 eV under these conditions. We conclude that the monochromator resolution is about a factor of two worse than theoretical above the oxygen edge. Scattered light was estimated to be about 20 percent in the region above the oxygen edge.<sup>7</sup>

The NPD on the S(2p) level (binding energy 170 eV with respect to the vacuum level) did not require dedicated time because, averaged over the energy range studied, the S(2p) cross section for c(2x2)S-Ni(001) is about five times as large as that of the O(1s) cross section for c(2x2)O-Ni(001). The stored ring current was 10–15 mA during this experiment. Measurement of the relative S(2p) intensity was severely hampered by the sharp dropoff in monochromatized light at and above the carbon K-edge (284 eV), due to absorption by

the carbon contamination on the optical elements of the monochromator. The photon flux was monitored continuously during these experiments by measuring the photoyield from a 90 percent transmitting gold mesh placed in the path of the beam.

The O(1s) and S(2p) differential (angle-resolved) relative intensities were mapped out by taking a series of low resolution ARP spectra normal to the (001) sample face in the region of the core level peak. A smooth background was subtracted before calculation of the peak area. The area was then adjusted for photon flux and analyzer transmission. Spectra were taken at intervals of 3 eV in photon energy to generate the NPD curve.

### III. RESULTS AND DISCUSSION

In spite of its poor resolution at the higher energies, the grasshopper monochromator, with a 1200 line/mm grating, provides adequate intensity and resolution to permit NPD studies on adsorbate core levels with binding energies in the 100–600 eV range. In this section we report separately on the oxygen and sulfur adsorbate systems.

#### A. The c(2x2) Oxygen Overlayer

In Fig. 1 we show the experimental NPD curve of the O(1s) level for the c(2x2)O overlayer on Ni(001) with the geometry shown in the inset. The curve was taken with the sample at room temperature, and was reproducible with an increased peak/valley ratio, after cooling the sample to 120 K. Peaks in the O(1s) intensity lie at the following kinetic energies (with respect to the vacuum level): 33, 62, 98, 118 (shoulder), 155, and 185 eV. Above the experimental curve in Fig. 1 are two theoretical curves corresponding to placing the oxygen atom in a fourfold hollow site above the nickel surface at  $d_{\perp} = 0.90\text{\AA}$  and  $d_{\perp} = 1.76\text{\AA}$ , respectively, where  $d_{\perp}$  is the spacing between the oxygen and the top layer of nickel atoms. These two theoretical curves show the closest agreement with our data of all  $d_{\perp}$  spacings tested (0.50  $\text{\AA}$  through 1.70  $\text{\AA}$  at intervals of 0.10  $\text{\AA}$ , and 1.76  $\text{\AA}$ ). Of these two, the lower curve ( $d_{\perp} = 0.90\text{\AA}$ ) clearly gives the best fit—three peaks match up almost exactly while two others differ by only 3 eV. In this geometry, the Ni-O bond length is 1.98  $\text{\AA}$  and the oxygen is situated above the fourfold hollow of the (001) surface with the oxygen and nickel hard-sphere radii just touching. The upper curve ( $d_{\perp} = 1.76\text{\AA}$ ) matches up fairly well with experiment below 100 eV kinetic energy but

has large peaks at 127 and 164 eV which do not correspond to any features in the experimental curve. Although it is physically unlikely that the oxygen atoms lie  $1.76\text{\AA}$  above the nickel surface, the NPD curve for this geometry is expected to be almost identical to that for a  $c(2 \times 2)$  oxygen overlayer coplanar with the nickel surface ( $d_{\perp} = 0\text{\AA}$ ). This is because the interlayer spacing in bulk nickel is  $1.76\text{\AA}$ , so that if the intralayer scattering due to the surface nickel atoms coplanar with the  $c(2 \times 2)$  oxygen structure is assumed to be small, one should get essentially the same scattering process as that for a  $c(2 \times 2)0$  overlayer at  $d_{\perp} = 0\text{\AA}$ . This is especially true of normal emission, where intralayer scattering occurs at a  $90^{\circ}$  angle from the emission direction. Unfortunately, the theoretical approach used in this work is not readily applicable to the  $d_{\perp} = 0\text{\AA}$  geometry, and a direct calculation of this geometry is therefore not yet available.

In order to estimate the accuracy of the  $d_{\perp}$  value determined by NPD, one must contend with uncertainties in both experiment and theory. The rms peak energy reproducibility in the experimental data is estimated to be  $\pm 1.0$  eV. The theoretical accuracy in peak energy position is more difficult to determine because of the use of the inner potential ( $V_0$ ) as a parameter in the calculation. The inner potential is roughly the average potential felt by an excited electron leaving the solid, so that a change in  $V_0$  produces a corresponding shift in the kinetic energy scale of an NPD theoretical curve. For this reason, the uncertainty in the theoretical data must be estimated by observing the shift in the energy difference between two peaks ( $\Delta E$ ) as a function of  $d_{\perp}$ , rather than the shift in absolute position of a

single peak. The rms shift in  $\Delta E$  is estimated to be 40 eV/Å for these data, and the experimental uncertainty in this quantity is  $\pm 1.5$  eV. This yields a value of  $\pm 0.04$  Å for the accuracy of the determination of  $d_{\perp}$  by NPD for the system  $c(2 \times 2)O(1s)-Ni(001)$ . With further improvements, an accuracy of  $\pm 0.01$  Å should be possible.

The  $c(2 \times 2)O-Ni(001)$  system has been the object of numerous studies with other techniques. Early LEED I-V studies, based on the data of Demuth and Rhodin,<sup>9</sup> gave evidence for three different structures. Andersson, et al.<sup>10</sup> and Demuth,<sup>11</sup> et al., found the oxygen to sit above the fourfold hollow site with  $d_{\perp}$  values of 1.5 Å and 0.9 Å, respectively. Duke, et al.,<sup>12</sup> concluded that the oxygen atoms form a reconstructed Ni-O square lattice which sits on the Ni(001) surface. In the past few years the structure predicted by Demuth, Jepsen and Marcus has become generally accepted; i.e., the  $c(2 \times 2)$  overlayer of oxygen atoms is believed to occupy the fourfold hollow site at  $d_{\perp} = 0.9$  Å.<sup>13,14</sup> Recently, rapid LEED intensity measurements by Hanke et al., have confirmed this structure.<sup>15</sup> Azimuthal photoelectron diffraction (APD) studies by Petersson et al.,<sup>16</sup> found that for a 15 L exposure of oxygen, which yielded a  $c(2 \times 2)$  LEED pattern, the oxygen was nearly coplanar ( $d_{\perp} = 0.1$  Å) with the nickel surface. Their data indicate that the oxygen sits 0.8–0.9 Å above the surface at low coverages (exposures less than 1 L) and then moves down into the nickel plane ( $d_{\perp} = 0.1$  Å) as the exposure is increased to 15 L, at which point they noted a  $c(2 \times 2)$  LEED pattern. This result is not consistent with ours, as the NPD data indicates that for a 20 L exposure and sharp  $c(2 \times 2)$  LEED pattern, the oxygen still sits 0.9 Å

above the surface. Stöhr<sup>17</sup> has studied a 40 L exposure of O<sub>2</sub> on Ni(001) with surface-EXAFS. His analysis yielded an O-Ni distance of 2.04 Å, and he concluded that his surface layer was essentially NiO, with a slight relaxation of the Ni-O bond distance, which is 2.08 Å in bulk NiO. Since Stöhr did not monitor the LEED pattern, the fractional coverage was uncertain. Stöhr did not report measurements with lower O<sub>2</sub> exposures, so a comparison with our c(2x2) results is not appropriate. Brongersma, et al.,<sup>18</sup> used ion scattering spectroscopy (ISS) to determine that oxygen sits in the fourfold hollow site, 0.9 Å above the surface. An electron energy loss spectroscopy (EELS) experiment by Andersson yielded vibrational losses of 53 and 39 meV for the p(2x2)O and c(2x2)O structures respectively.<sup>19</sup> Andersson attributed the large change (14 meV) in energy loss to the low potential energy barrier for oxygen chemisorption. Finally, we discuss some x-ray photoelectron spectroscopy (XPS) work on this system. Two O(1s) features have been observed; one at about 529.5 eV below the Fermi level and a smaller near 531 eV, but the interpretation of the spectra has differed.<sup>8,20,21</sup> According to Brundle,<sup>21</sup> it is now generally agreed that the peak at 529.5 eV can be characteristic of both the chemisorbed oxygen overlayer and of oxygen in NiO. This indicates that XPS will not be sensitive to a change in the position of the oxygen with respect to the surface. The higher binding energy peak appears after large (>100 L) exposures of O<sub>2</sub>, and its origin is uncertain. Similarly, the Ni 2p<sub>3/2</sub> level observed at a binding energy of 852.8 eV does not experience a significant adsorbate-induced energy shift except for very high coverages of oxygen.

The wide variety of results obtained for the structure of  $c(2 \times 2)0$  on Ni(001) is not surprising if one considers the different exposures and conditions which have been used to produce the  $c(2 \times 2)$  overlayers. In our experiment, the  $c(2 \times 2)$  LEED pattern became sharp at 20 L exposure. The  $c(2 \times 2)$  pattern has been shown to persist over the range of exposures up to 100 L, but there is evidence of significant NiO island formation at this coverage.<sup>8,22</sup> Consequently, the interaction of the Ni(001) surface with oxygen changes from chemisorption to oxidation while the  $c(2 \times 2)$  structure is present, at which point the oxygen has moved into the plane. The APD data<sup>16</sup> indicate that the oxygen moves down after a 15 L exposure even before the last evidence of a  $p(2 \times 2)$  pattern is gone. However, the APD technique is much more sensitive to atomically adsorbed oxygen in or below the surface than to oxygen lying well above the surface. This is because there is a low probability at XPS energies for scattering at angles more than a few degrees from the forward direction.<sup>23</sup> Thus, even though a  $c(2 \times 2)$  overlayer may be predominant, a small amount of oxygen present in the surface plane could strongly affect the angular dependence of the angle-resolved XPS cross section and resultant surface structure determination. Clearly, the possibility of multiple chemisorption sites cannot be ruled out for a  $c(2 \times 2)0$  coverage, especially at higher exposures (>40 L), where a transition from above plane to coplanar oxygen atoms occurs. Our NPD data, however, indicate that upon the first evidence of a clear  $c(2 \times 2)$  LEED pattern at 20 L  $O_2$  exposure, most of the oxygen lies above the fourfold hollows.

We conclude this subsection with two observations. First, the NPD and APD results may be consistent. A small fraction of oxygen atoms at  $d_{\perp} = 0.1\text{\AA}$  might go unnoticed in the NPD data but be dominant in APD. Also, our NPD data do not directly rule out  $d_{\perp} = 0.1\text{\AA}$ , for which no NPD calculations exist. Second, it may not be necessary to reconcile the data, which were taken on different samples. Combined NPD, APD, and surface-EXAFS studies on one sample would be desirable.

#### B. The c(2x2) Sulfur Overlayer

The second system which we will consider in this paper is the c(2x2) sulfur overlayer on Ni(001). An NPD curve for this system, extending up to 100 eV above the S(2p) edge, has already been published.<sup>1</sup> Here we present a more extensive NPD curve (up to 200 eV kinetic energy) as well as calculations for the three symmetric adsorption sites. Since the sulfur atom has a larger atomic radius than oxygen, it is believed to reside completely above the Ni(001) surface in the submonolayer regime. The experimental NPD curve is shown in Fig. 2, for the geometry shown in the inset. The measurements were made after cooling the c(2x2)S-Ni(001) sample (prepared at 300 K) to 120 K. Just as in the case of the oxygen overlayer, the NPD curve taken after cooling to 120 K had an increased peak/valley ratio, but essentially the same peak energies and relative intensities. The theoretical calculations shown are for the fourfold hollow site ( $d_{\perp} = 1.30\text{\AA}$ ), the twofold bridge site ( $d_{\perp} = 1.80\text{\AA}$ ) and atop site ( $d_{\perp} = 2.19\text{\AA}$ ). As was the case in oxygen, the best agreement between theory and experiment is found to be the fourfold hollow site ( $d_{\perp} = 1.30\text{\AA}$ ) on the (001) surface. Using the method described in the previous sub-



section, the accuracy of the  $d_1$  value determined for the sulfur is  $\pm 0.04\text{\AA}$ , the same as in the oxygen case. The agreement is quite poor for the other two sites. Four of the peaks calculated for the four-fold hollow site match experimental peaks to within 1 eV. The only disagreement is in the low kinetic energy region, where the experimental peak at 35 eV does not match the calculated peak at 40 eV. In this region, the calculated peak positions are very sensitive to the choice of the sulfur scattering potential, whereas all other calculated peak positions (57, 82, 129, and 172 eV) are fairly insensitive to that potential. The theory also does not address the predominance of multiple scattering and other effects close to the edge. We note that above 50 eV kinetic energy, all of these complications become more manageable, and the experiment-theory agreement improves dramatically. The relative intensities of the experimental peaks, as well as their positions, are closely reproduced by the theory.

The  $c(2\times 2)\text{S-Ni}(001)$  system has been the subject of several earlier structural studies. An ARP study by Plummer et al.<sup>24</sup> on the  $\text{S}(3p)$  derived level for this system found a resonance peak at  $h\nu=18$  eV. This peak was reproduced by Li and Tong's calculations only if the sulfur atoms were placed in fourfold hollow sites at  $d_1 = 1.30\text{\AA}$ .<sup>25</sup> The first LEED intensity analyses concluded that the sulfur is situated above the surface in the fourfold hollow site, although there was disagreement as to whether  $d_1$  was  $1.3\text{\AA}$ ,<sup>11,26</sup> (the hard-sphere radius result) or  $1.7\text{\AA}$ .<sup>12</sup> As in the case of the corresponding oxygen

system discussed above, the hard-sphere radius result<sup>13,14</sup> was eventually agreed upon, and a recent experimental and theoretical study using iso-intensity maps of specular beam data confirmed that structure.<sup>27</sup>

#### IV. FOURIER TRANSFORM ANALYSIS

Our experimental data were compared to calculations in Section III. The calculations utilize a multiple-scattering approach to ultraviolet and soft x-ray photoemission spectroscopy.<sup>4</sup> The initial state is calculated by choosing a cluster of atoms representing the postulated geometry of nickel atoms about the sulfur or oxygen adsorbate and solving for the cluster wave function using the  $X\alpha$  scattered-wave method. The final-state scattering is modeled by using a multiple-scattering T matrix to propagate the photoelectron wave through the first few surface layers. Recently, Li and Tong have developed a simplified scheme, called the quasi-dynamical (QD) method, which produced very accurate intensity versus electron kinetic energy curves for energies greater than 60 eV when compared to the full dynamical calculation.<sup>28</sup> The QD calculation takes advantage of the fact that in the high-energy limit, forward scattering is the predominant process. The only scattering events considered besides all forward scatterings are (a) one backscattering from each layer, and (b) one scattering from each atom within a layer. All NPD calculations shown here utilize the full dynamical method, but the results of the quasi-dynamical method give consistent results. Unfortunately, even the QD approach is quite involved, and comparison with experiment is implicit.

To avoid the complexities of the calculations, we have searched for simpler methods of analyzing NPD data. The kinematical method, which assumes that single-scattering is the predominant factor, has

been tried without much success on the system  $p(2 \times 2)\text{Se-Ni}(001)$ . Li and Tong have done a kinematical calculation on that system in the kinetic energy range 150–400 eV and found substantial disagreement with their dynamical calculations over that energy range.<sup>28</sup> It is clear that in this energy regime, multiple scattering cannot be ignored.

Another method which we have considered is the use of the Fourier transform to isolate the single scattering effects. The Fourier transform has been used with great success in interpreting extended x-ray absorption fine structure (EXAFS) data.<sup>29</sup> In EXAFS, the final-state electron scattering intensity is isolated from the atomic-like initial state background by determining the function  $X(k) = (I - I_0)/I_0$ , where  $I$  is the total absorption and  $I_0$  is a smooth atomic background. If the phase shift of the scattering atoms is independent of energy, then the Fourier transform has been shown to yield interatomic distances rigorously for  $s$  initial states, and approximately for other states under certain conditions.<sup>30</sup> Since EXAFS is an angle-integrated technique, it yields the nearest-neighbor distances from the central excited atom. By analogy, one might expect intuitively that a Fourier transform of NPD data would be sensitive to the one-dimensional structure normal to the crystal face, as NPD is an angle-resolved technique. Recently, our group has applied the Fourier transform technique to NPD curves calculated by Li and Tong for the  $(\sqrt{3} \times \sqrt{3}) R30^\circ \text{Se-Ni}(111)$  system, with much success. Details of the results, as well as discussion of the theoretical justification for

applying the Fourier transform method to NPD, will be published elsewhere.<sup>31</sup>

One of the criteria for a successful transform of EXAFS data is the need for an extended  $k$ -space data set. Typical EXAFS spectra extend from about 50 eV to a few hundred eV above the absorption edge. If the range of  $k$ -space data is too small, the Fourier transform may not be able to pick up a sufficient number of oscillations to yield accurate structural information. In particular, if the experimental data do not extend far enough above the edge, the low  $R_{nn}$  peaks in the Fourier transformed data may be lost.

With this limitation in mind, we nevertheless carried out fast Fourier transforms of the function  $\chi(k) = (I - I_0)/I_0$  for these NPD curves. The range of data used for both the O(1s) in c(2x2)O-Ni(001) and the S(2p) in c(2x2)S-Ni(001) cases was  $50 \text{ eV} < E_{kin} < 200 \text{ eV}$ , or roughly  $4 \text{ \AA}^{-1} < k < 7.5 \text{ \AA}^{-1}$ . Since the phase shifts in the NPD process have been predicted to be much smaller than those in EXAFS,<sup>31</sup> they were omitted for these initial calculations. The inclusion of best estimates of phase shifts would change the location of the peaks in the real space distribution function by less than  $0.05 \text{ \AA}$ .<sup>31</sup> Care was taken to terminate the data at points where  $\chi(k) = 0$ . The transform was found to be fairly insensitive to changes in the estimated atomic background  $I_0$ .

In Fig. 3, we show the function  $\chi(k)$  for c(2x2)S(2p)-Ni(001). Note that the large modulations in  $\chi(k)$  (-0.4 to 0.4) for NPD are an order of magnitude greater than those typical in EXAFS. These large

modulations make the analysis much less sensitive to the background subtraction. Due to experimental limitations such as the  $1/E_{\text{kin}}$  dependence of the analyzer transmission function and the performance of the grasshopper monochromator at high photon energies (discussed above), the measurements were only taken up to 200 eV above threshold. In addition, the scattering cross-sections are decreasing functions of energy above 200 eV, resulting in a substantial reduction in the size of the modulations. The modulus of the Fourier transform is shown in Fig. 4. There are two major peaks, showing maxima at 3.02 and 4.83Å. NPD and LEED analyses yield  $d_{\perp} = 1.30\text{Å}$ , and the interlayer spacing for Ni(001) is  $b = 1.76\text{Å}$ . These two peaks are therefore attributed to the distances  $d_{\perp} + b = 3.06\text{Å}$  and  $d_{\perp} + 2b = 4.82\text{Å}$ . There is no peak in the real-space distribution function for  $d_{\perp} = 1.3\text{Å}$ , probably because our NPD data does not extend to high enough  $k$  values. The agreement for the two main peaks is very good considering the limited data range.

The Fourier transform technique was also applied to the NPD curve for  $c(2 \times 2)0(1s)\text{-Ni}(001)$ . The function  $X(k)$  is shown in Fig. 5, and the corresponding transform in Fig. 6. For this system, NPD and LEED give  $d_{\perp} = 0.90\text{Å}$ , from which  $d_{\perp} + b = 2.66\text{Å}$ , and  $d_{\perp} + 2b = 4.42\text{Å}$ . Again, we find that the two main peaks in the transformed data, at 2.70 and 4.33Å, match up fairly close with these previously determined values of  $d_{\perp} + b$  and  $d_{\perp} + 2b$ . Although there is a peak at 0.82Å, it is too small to be considered as the  $d_{\perp}$  peak.

These two examples support the idea that Fourier transformation of NPD data yields structural information directly, but they do not prove it. There are two ingredients lacking in establishing Fourier transform NPD as a viable data-analysis technique. First, a convincing theoretical analysis would be needed of why peaks in the Fourier transform fall at the perpendicular interplanar distances  $d_{\perp} + nb$ ,  $n = 0, 1, 2, \dots$ . Second, the experimental range of the data set should be expanded to higher  $k$  values, to yield a peak at the  $d_{\perp}$  distance itself, in addition to  $d_{\perp} + b$ ,  $d_{\perp} + 2b$ , etc. We do not regard this latter requirement as absolutely essential in general, but it should at least be demonstrated for one or more prototype systems.

## V. CONCLUSIONS

The normal emission photoelectron diffraction technique was used to determine that the  $c(2 \times 2)0$  and  $c(2 \times 2)S$  overlayers on Ni(001) sit above the fourfold hollow site in the surface with  $d_{\perp}$  spacings of  $0.90 \pm 0.04 \text{ \AA}$  and  $1.30 \pm 0.04 \text{ \AA}$ , respectively. These distances agree with LEED results. More work on the oxygen-nickel system as a function of coverage is needed to more fully understand the transition from chemisorbed oxygen to bulk nickel oxide. A coverage-dependent surface-EXAFS study of this system would also be of interest. The similarity between NPD and EXAFS has been further confirmed by applying the Fourier transform technique to experimental NPD data. There is a clear need for a theoretical framework to explain why these transforms are successful. Experimentally, there is a need to carry out the NPD measurements to at least 400 eV above the absorption edge. Experiments are being planned for the new crystal monochromator beam line at SSRL, which will circumvent the problems of the grasshopper monochromator.



## ACKNOWLEDGMENTS

We wish to acknowledge Mrs. Winifred Heppler for the preparation of the nickel crystal.

This work was performed by the Division of Chemical Sciences, Office of Basic Energy Sciences, U. S. Department of Energy under Contract No. W-7405-ENG-48. It was performed at the Stanford Synchrotron Radiation Laboratory, which is supported by the NSF Grant No. DMR 77-27489, in cooperation with the Stanford Linear Accelerator Center. One of us (J.G.T.) acknowledges support by an NSF Predoctoral Fellowship.

## REFERENCES

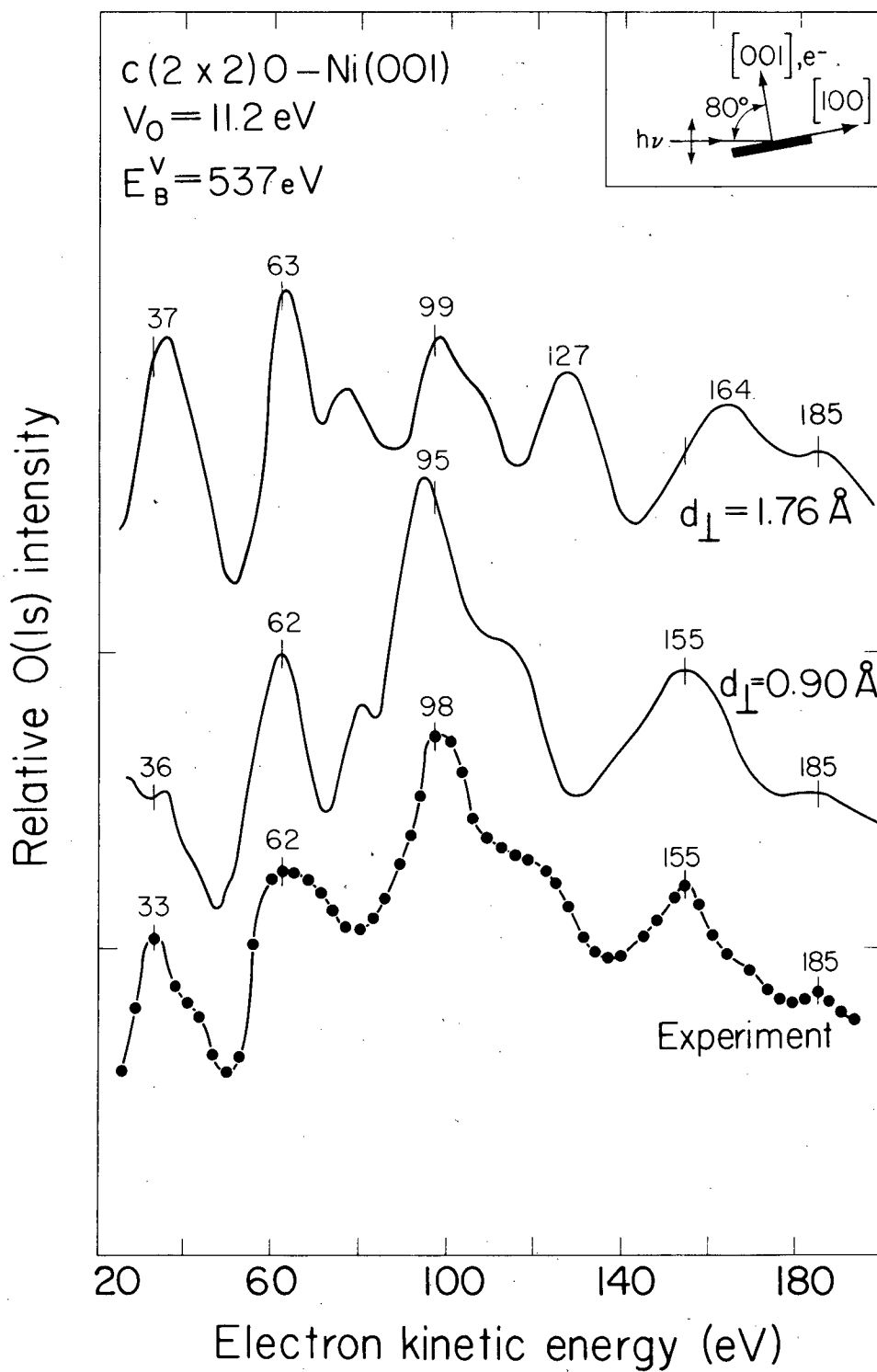
1. S. D. Kevan, D. H. Rosenblatt, D. Denley, B.-C. Lu, and D. A. Shirley, Phys. Rev. Lett. 41, 1565 (1978); Phys. Rev. B 20, 4133 (1979).
2. G. P. Williams, F. Cerrina, I. T. McGovern, and G. J. Lapeyre, Solid State Commun. 31, 15 (1979).
3. S. D. Kevan, R. F. Davis, D. H. Rosenblatt, J. G. Tobin, M. G. Mason, D. A. Shirley, C. H. Li, and S. Y. Tong, to be published.
4. C. H. Li, A. R. Lubinsky, and S. Y. Tong, Phys. Rev. B 17, 3128 (1978).
5. S. D. Kevan, J. G. Tobin, D. H. Rosenblatt, R. F. Davis, and D. A. Shirley, to be published.
6. C. H. Li and S. Y. Tong, Phys. Rev. Lett. 42, 901 (1979).
7. S. D. Kevan, Ph. D. Thesis, University of California, Berkeley (1980), (unpublished); S. D. Kevan and D. A. Shirley, Phys. Rev. B 22, 542 (1980).
8. T. Fleisch, N. Winograd, and W. N. Delgass, Surf. Sci. 78, 141 (1978).
9. J. E. Demuth and T. N. Rhodin, Surf. Sci. 45, 249 (1974).
10. S. Andersson, B. Kasemo, J. B. Pendry, and M. A. Van Hove, Phys. Rev. Lett. 31, 595 (1973).
11. J. E. Demuth, D. W. Jepsen, and P. M. Marcus, Phys. Rev. Lett. 31, 540 (1973).
12. C. B. Duke, N. O. Lipari, and G. E. Laramore, Nuovo Cemento 23B, 241 (1974).

13. P. M. Marcus, J. E. Demuth, and D. W. Jepsen, Surf. Sci. 53, 501 (1975).
14. M. Van Hove and S. Y. Tong, J. Vac. Sci. Technol. 12, 230 (1975).
15. G. Hanke, E. Lang, K. Heinz, and K. Müller, Surf. Sci. 91, 551 (1975).
16. L.-G. Petersson, S. Kono, N. F. T. Hall, S. Goldberg, J. T. Lloyd, C. S. Fadley, and J. B. Pendry, Matl. Sci. and Engr. 42, 111 (1980).
17. J. Stöhr, private communication, August 1980.
18. H. H. Brongersma and J. B. Theeten, Surf. Sci. 54, 519 (1976).
19. S. Andersson, Surf. Sci. 79, 385 (1979).
20. N. G. Krishnan, W. N. Delgass, and W. D. Robertson, Surf. Sci. 57, 1 (1976).
21. C. R. Brundle and H. Hopster; presented at ICSS 4/ECOSS 3, Cannes, France (1980).
22. P. H. Holloway and J. B. Hudson, Surf. Sci. 43, 123 (1974).
23. S. Kono, S. M. Goldberg, N. F. T. Hall, and C. S. Fadley, to appear in Phys. Rev. B.
24. E. W. Plummer, B. Tonner, N. Holzwarth, and A. Liebsch, Phys. Rev. B 21, 4306 (1980).
25. C. H. Li and S. Y. Tong, Phys. Rev. Lett. 40, 46 (1978).
26. J. E. Demuth, D. W. Jepsen, and P. M. Marcus, Phys. Rev. Lett. 32, 1182 (1974).
27. Y. Gauthier, D. Aberdam, and R. Baudoing, Surf. Sci. 78, 339 (1978).
28. C. H. Li and S. Y. Tong, Phys. Rev. Lett. 43, 526 (1979).

29. E. A. Stern, D. E. Sayers, and F. W. Lytle, Phys. Rev. B. 11, 4836 (1975).
30. A. Liebsch, Phys. Rev. B 13, 544 (1976).
31. Z. Hussain, D. A. Shirley, C. H. Li, and S. Y. Tong, to be published.
32. G. D. Bergland, IEEE Spect. July, 41 (1969).

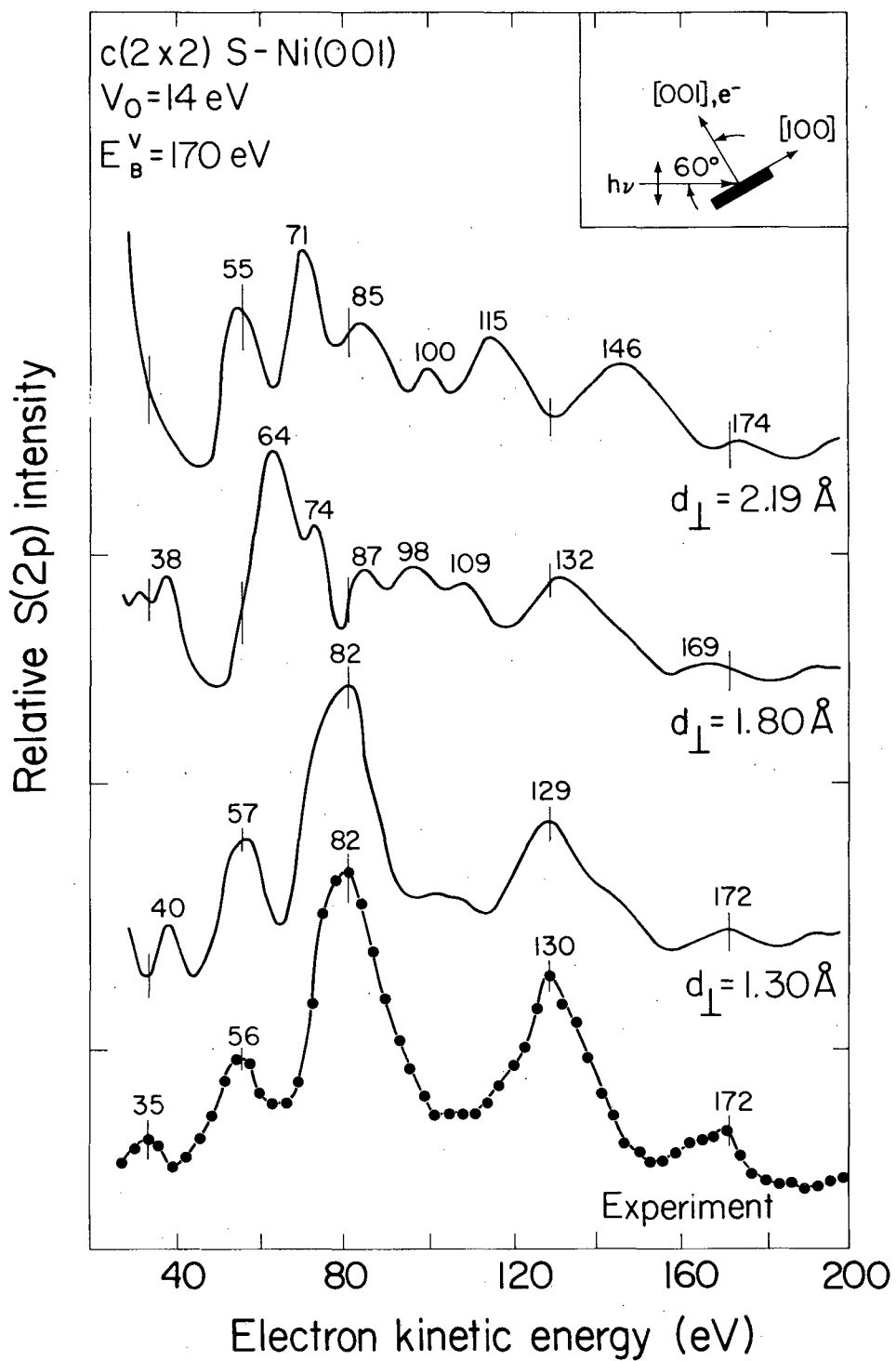
## FIGURE CAPTIONS

- Fig. 1. NPD curve for O(1s) electrons from c(2x2)O-Ni(001), compared with theoretical curves for  $d_1 = 0.90$  and  $1.76\text{\AA}$  for the experimental geometry shown. The binding energy for O(1s) is 537 eV with respect to the vacuum level. The inner potential in the calculation is 11.2 eV.
- Fig. 2. NPD curve for S(2p) electrons from c(2x2)S-Ni(001), compared with theoretical curves for  $d_1 = 1.30, 1.80,$  and  $2.19\text{\AA}$  for the experimental geometry shown. The binding energy for S(2p) is 170 eV with respect to the vacuum level. The inner potential in the calculation is 14 eV.
- Fig. 3. Plot of  $\chi(k) = (I - I_0)/I_0$  for S(2p) NPD data for c(2x2)S-Ni(001).
- Fig. 4. Magnitude of the Fourier transform of the data in Fig. 3.
- Fig. 5. Plot of  $\chi(k) = (I - I_0)/I_0$  for O(1s) NPD data for c(2x2)O-Ni(001).
- Fig. 6. Magnitude of the Fourier transform of the data in Fig. 5.



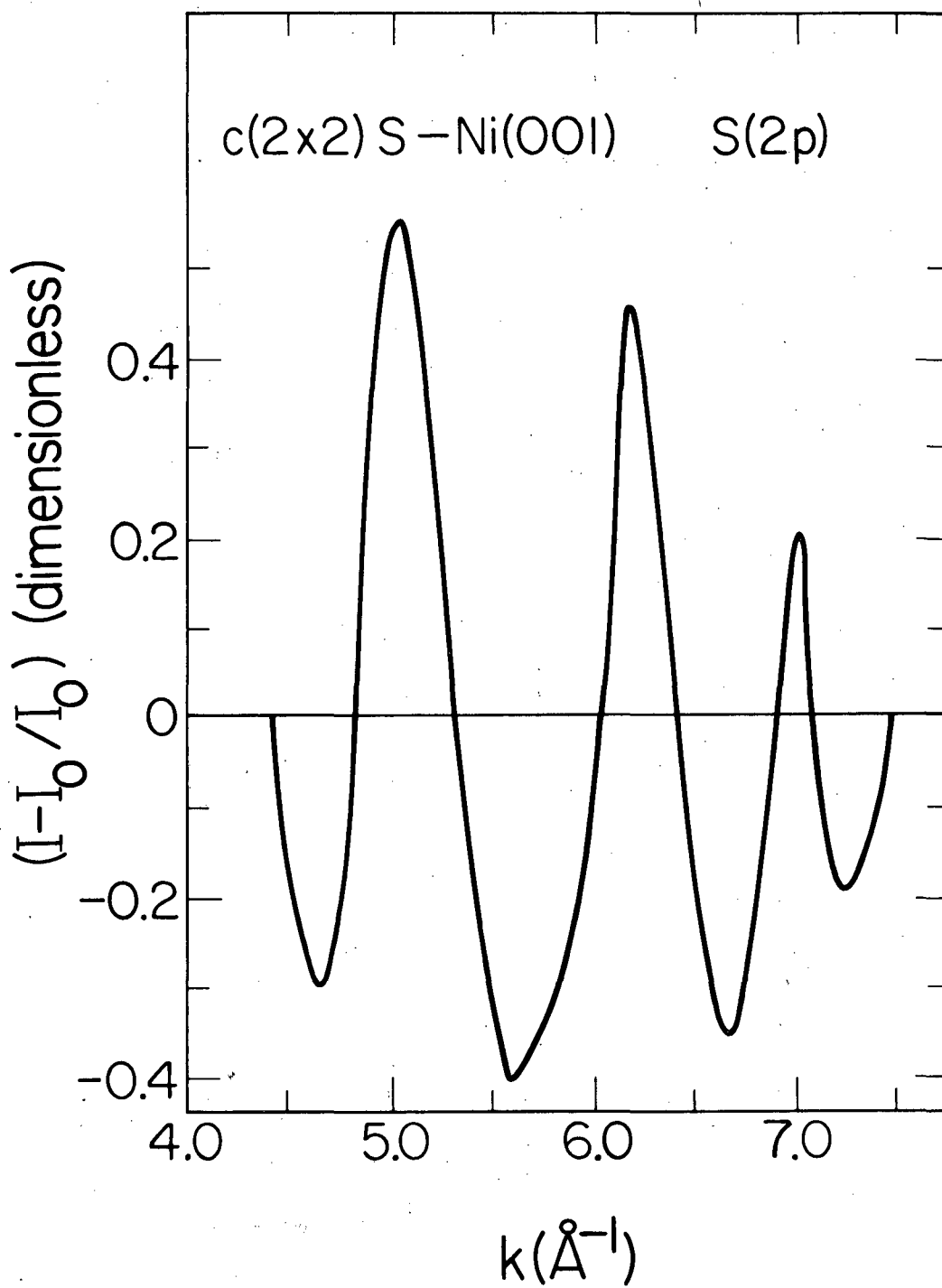
XBL8010-2112

Figure 1



XBL8010-2113

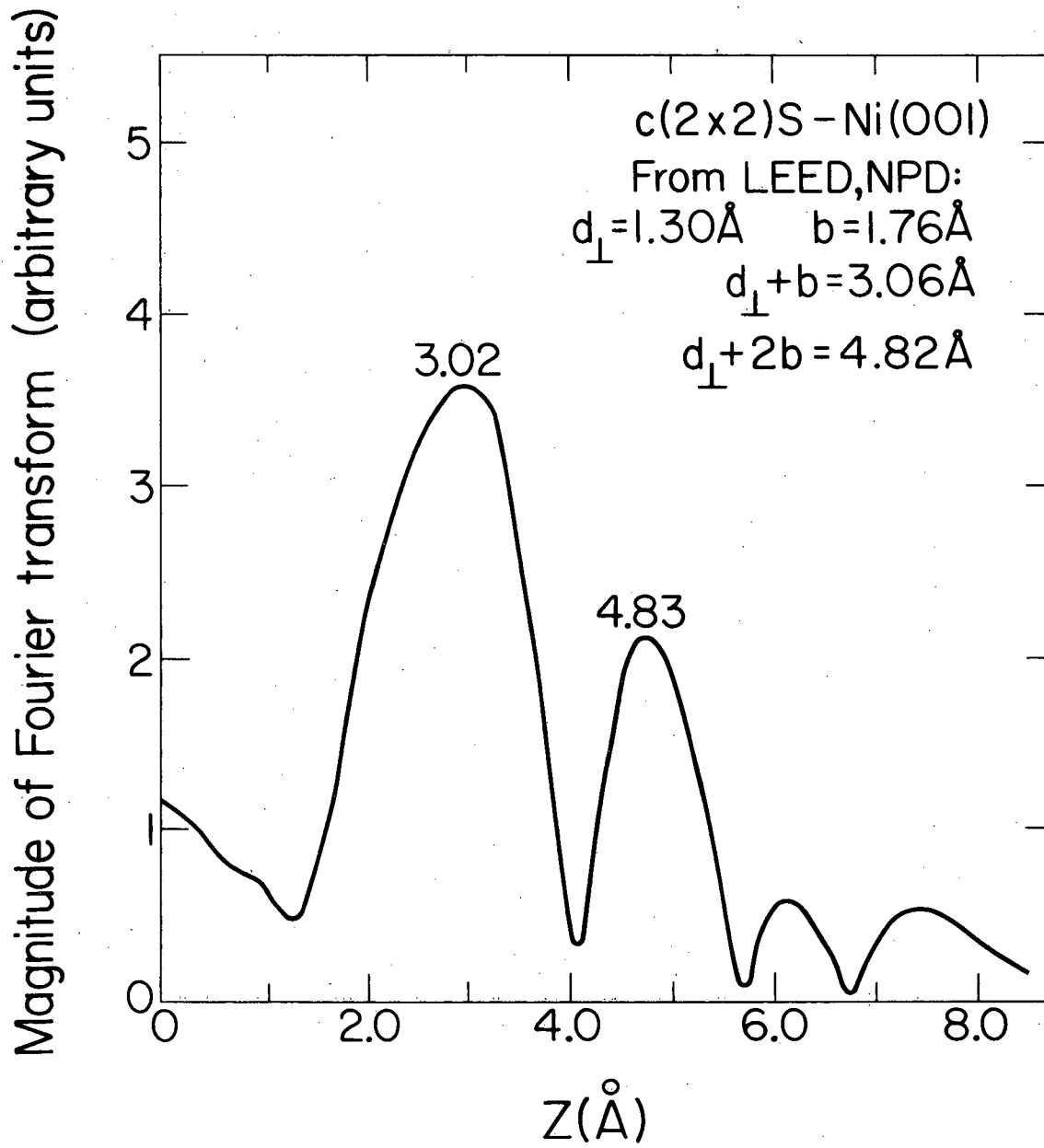
Figure 2



XBL 8010-2114

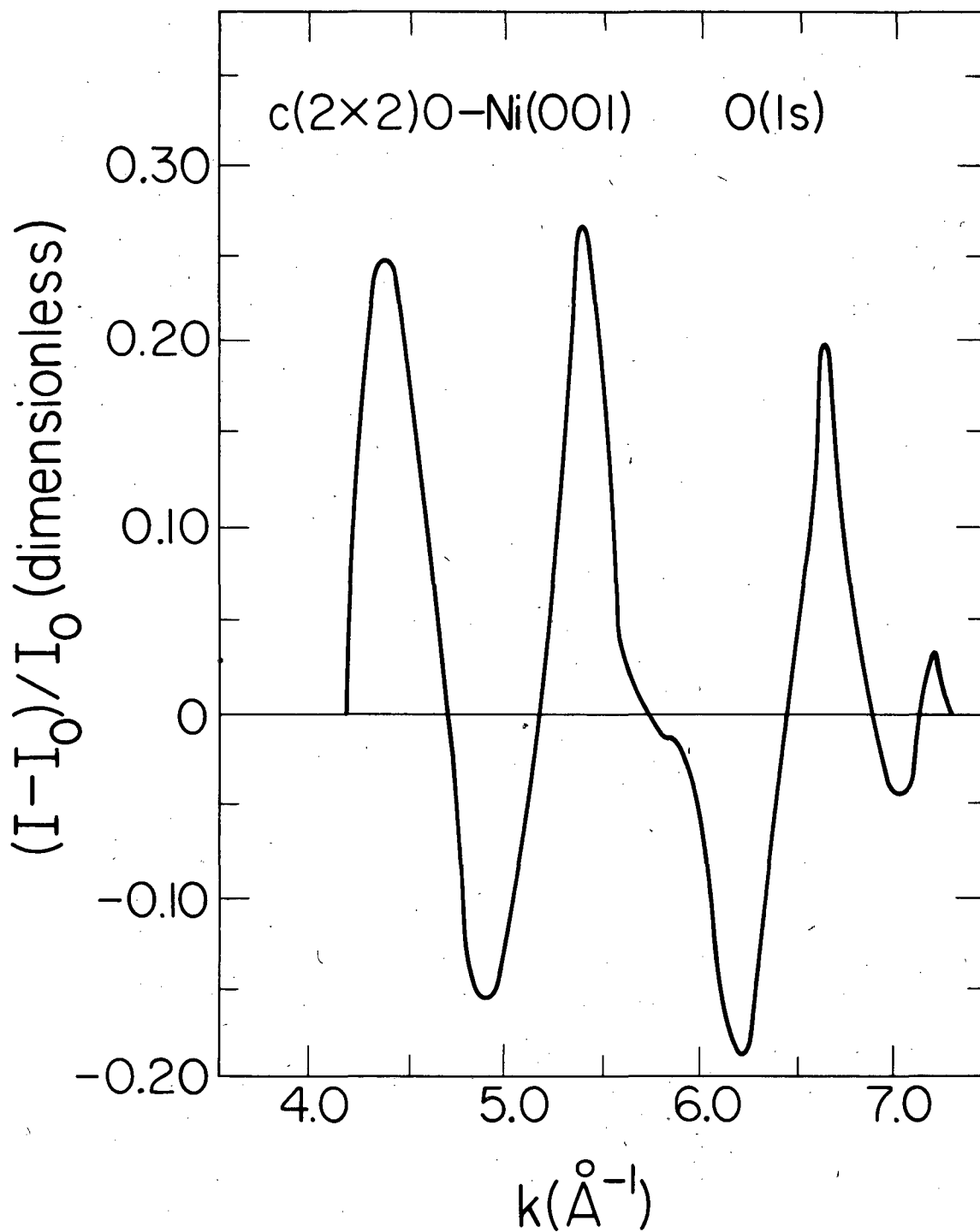
Figure 3





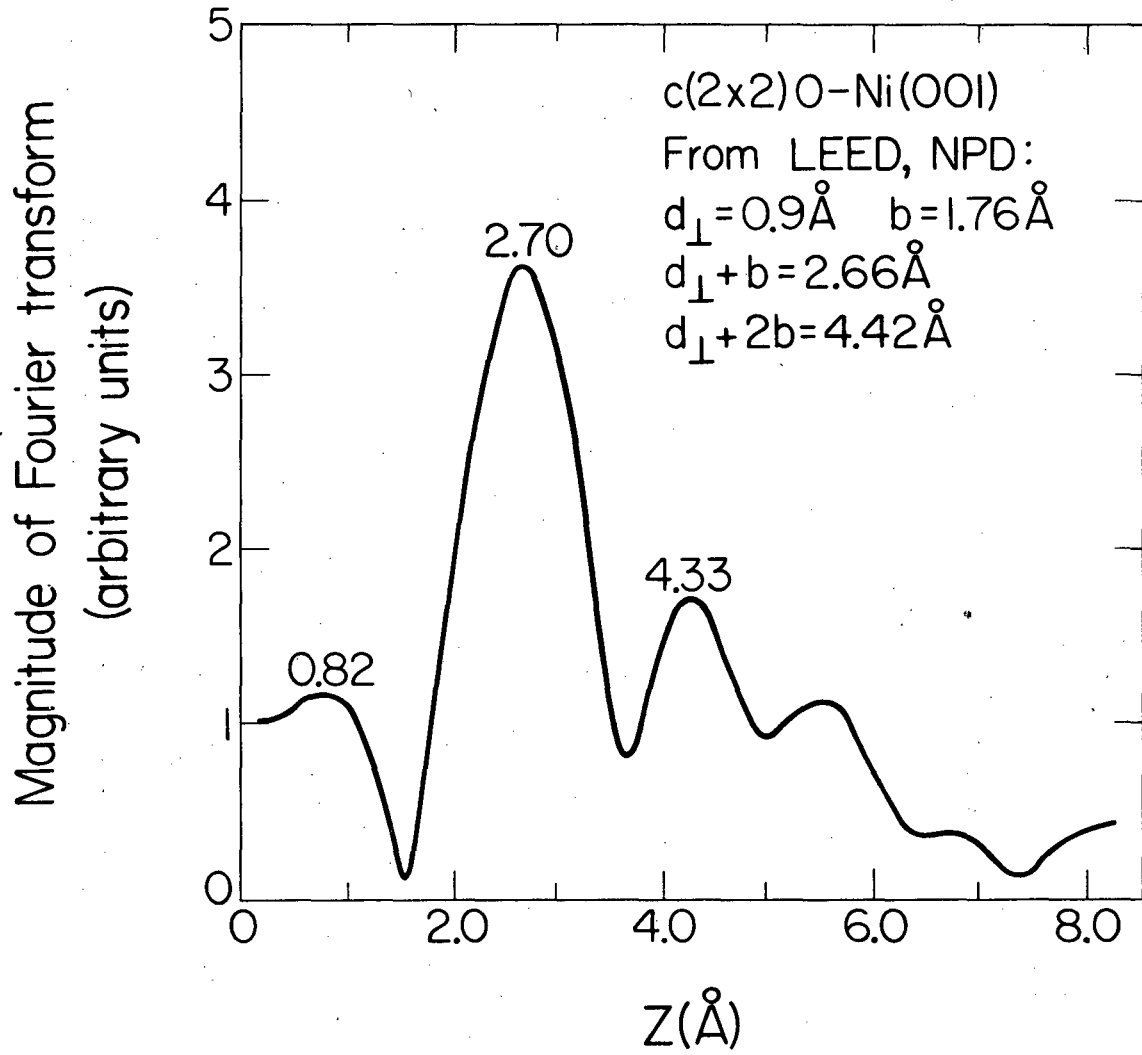
XBL8010 - 2116

Figure 4



XBL 8010 - 2115

Figure 5



XBL8010-2117

Figure 6

This report was done with support from the Department of Energy. Any conclusions or opinions expressed in this report represent solely those of the author(s) and not necessarily those of The Regents of the University of California, the Lawrence Berkeley Laboratory or the Department of Energy.

Reference to a company or product name does not imply approval or recommendation of the product by the University of California or the U.S. Department of Energy to the exclusion of others that may be suitable.

TECHNICAL INFORMATION DEPARTMENT  
LAWRENCE BERKELEY LABORATORY  
UNIVERSITY OF CALIFORNIA  
BERKELEY, CALIFORNIA 94720